



Published in final edited form as:

*Arch Biochem Biophys.* 2018 November 01; 657: 1–7. doi:10.1016/j.abb.2018.08.013.

## Analyzing the Function of the Insert Region Found Between the $\alpha$ and $\beta$ -Subunits in the Eukaryotic Nitrile Hydratase from *Monosiga brevicollis*

Xinhang Yang<sup>1</sup>, Brian Bennett<sup>2</sup>, and Richard C. Holz<sup>1,\*</sup>

<sup>1</sup>Department of Chemistry, Marquette University, PO Box 1881, Milwaukee, Wisconsin 53201

<sup>2</sup>Department of Physics, Marquette University, PO Box 1881, Milwaukee, Wisconsin 53201-1881s

### Abstract

The functional roles of the (His)<sub>17</sub> region and an insert region in the eukaryotic nitrile hydratase (NHase, EC 4.2.1.84) from *Monosiga brevicollis* (*Mb*NHase), were examined. Two deletion mutants, *Mb*NHase<sup>238–257</sup> and *Mb*NHase<sup>219–272</sup>, were prepared in which the (His)<sub>17</sub> sequence and the entire insert region were removed. Each of these *Mb*NHase enzymes provided an  $\alpha_2\beta_2$  heterotetramer, identical to that observed for prokaryotic NHases and contains their full complement of cobalt ions. Deletion of the (His)<sub>17</sub> motif provides an *Mb*NHase enzyme that is ~55% as active as the WT enzyme when expressed in the absence of the Co-type activator (*e*) protein from *Pseudonocardia thermophila* JCM 3095 (*Pt*NHase<sup>act</sup>) but ~28% more active when expressed in the presence of *Pt*NHase<sup>act</sup>. *Mb*NHase<sup>219–272</sup> exhibits ~55% and ~89% of WT activity, respectively, when expressed in the absence or presence of *Pt*NHase<sup>act</sup>. Proteolytic cleavage of *Mb*NHase provides an  $\alpha_2\beta_2$  heterotetramer that is modestly more active compared to WT *Mb*NHase ( $k_{\text{cat}} = 163 \pm 4$  vs  $131 \pm 3$  s<sup>-1</sup>). Combination of these data establish that neither the (His)<sub>17</sub> nor the insert region are required for metalcentre assembly and maturation, suggesting that Co-type eukaryotic NHases utilize a different mechanism for metal ion incorporation and post-translational activation compared to prokaryotic NHases.

### Keywords

Nitrile hydratase; enzyme kinetics; cobalt; protein biosynthesis; metal transport; metal insertion

### Introduction

Nitrile hydratases (NHases, EC 4.2.1.84) are metalloenzymes that contain either a non-heme Fe(III) ion (Fe-type) or a non-corrin Co(III) ion (Co-type) in their active site [1, 2]. NHases

\*To whom correspondence should be addressed: Richard C. Holz, Department of Chemistry, Marquette University, PO Box 1881, Milwaukee, WI 53201, Phone (414) 288-7230, richard.holz@marquette.edu.

**Publisher's Disclaimer:** This is a PDF file of an unedited manuscript that has been accepted for publication. As a service to our customers we are providing this early version of the manuscript. The manuscript will undergo copyediting, typesetting, and review of the resulting proof before it is published in its final citable form. Please note that during the production process errors may be discovered which could affect the content, and all legal disclaimers that apply to the journal pertain.

**Supporting Information.** Supplementary information includes the gene design for the *Mb*NHase<sup>238–257</sup> mutant (Figure SI-1) and an EPR spectrum of WT *Mb*NHase (Figure SI-2).

catalyze the hydration of nitriles to their corresponding higher value amides under mild conditions (room temperature and physiological pH) and have attracted substantial interest as biocatalysts in preparative organic chemistry and bioremediation processes [3–8]. NHases have historically been only found in prokaryotes; however, multiple eukaryotic organisms were shown to contain genes that potentially encode NHase enzymes [9, 10]. We recently cloned and over-expressed the candidate gene from the eukaryotic organism *Monosiga brevicollis* in *E. coli* and characterized a fully functional Co-type NHase gene product, with fused  $\alpha$ - and  $\beta$ -subunits linked by a (His)<sub>17</sub> containing region (*MbNHase*) (Figure 1) [11]. Size-exclusion chromatography indicated that *MbNHase* is an ( $\alpha\beta$ )<sub>2</sub> homodimer in solution, analogous to the  $\alpha_2\beta_2$  heterotetrameric architecture of prokaryotic NHases, of which numerous X-ray crystal structures exist [1, 2, 12, 13].

Several open reading frames (ORFs) have been identified just downstream from the structural  $\alpha$ - and  $\beta$ -subunit genes in prokaryotic NHases, and one of these genes has been proposed to function as an activator (*e*) protein [14–16]. The prevailing dogma is that both Co- and Fe-type NHase enzymes require the co-expression of an (*e*) protein to be fully metallated, post-translationally modified, and fully functional [14–16]. No such (*e*) protein has been identified for eukaryotic NHases, such as *MbNHase* [9, 10]. It is tempting to speculate that the insert region within *MbNHase*, which contains a (His)<sub>17</sub> motif, plays the role of the (*e*) protein. Histidine rich regions are present in some cobalamin (vitamin B12) biosynthetic pathway proteins, *e.g.*, the chelatase CbiX enzyme from *Bacillus megaterium* and CobW from *Pseudomonas denitrificans* [17]. Histidine rich regions are also found in accessory proteins involved in metalcentre assembly of nickel hydrogenases and ureases, such as HypB from *Bradyrhizobium japonicum* and *Rhizobium leguminosarum*, SlyD from *Escherichia coli* and *Helicobacter pylori*, UreE from *Klebsiella aerogenes*, and Hpn and Hpn-like proteins from *Helicobacter pylori* [18].

To investigate metalcentre assembly in *MbNHase*, we created three different altered *MbNHase* enzymes. First, we obtained a proteolytically cleaved *MbNHase* enzyme in which the  $\alpha$ - and  $\beta$ -subunits were separated providing an enzyme that structurally mimics prokaryotic NHase enzymes. Second, a mutant *MbNHase* enzyme, in which the entire (His)<sub>17</sub> motif was removed (*MbNHase*<sup>238–257</sup>), was constructed and expressed in the presence and absence of the prototypical prokaryotic Co-type (*e*) activator protein from *Pseudonocardia thermophila* JCM 3095 (*PtNHase*<sup>act</sup>). Finally, a mutant was constructed in which the entire insert region was deleted (*MbNHase*<sup>219–272</sup>), leaving only the classical prokaryotic NHase  $\alpha$ - and  $\beta$ -subunit analogs; this mutant was also expressed in the presence and absence *PtNHase*<sup>act</sup>. Functional interrogation of these species provides important insight into the role of the insert region in *MbNHase* and how eukaryotic NHase enzymes are metallated and post-translationally modified.

## Materials and Methods

### Materials.

Acrylonitrile, 2-Amino-2-hydroxymethyl-propane-1,3-diol (Tris-HCl), and 4-(2-hydroxyethyl)piperazine-1-ethanesulfonic acid (HEPES) were obtained from Sigma-

Aldrich. Oligonucleotides and genes were obtained from Integrated DNA Technologies, Inc. All other reagents were purchased commercially and were the highest purity available.

### Expression and Purification of MbNHase.

Protein sequences for the  $\alpha$ - and  $\beta$ -subunit genes of the putative WT *MbNHase* were obtained from ORF 37534 (UniProt ID A9V2C1.1) of *M. brevicollis* and the predicted gene was synthesized by Integrated DNA Technologies, Inc. with optimized *E. coli* codon usage. This gene was cloned into the kanamycin resistant pET21a<sup>+</sup> (EMD Biosciences) expression vector to create the plasmid pSMM0 $\alpha\beta$ , as previously reported [11].

A single colony was used to inoculate separate starter cultures of 50 mL LB Miller media containing the appropriate antibiotics (pET28a+: 50 mg/mL kanamycin) and allowed to grow at 37 °C with constant shaking overnight. These cultures were used to inoculate 6 L of LB Miller media containing the appropriate antibiotics and allowed to grow at 37 °C with constant shaking until an optical density of ~0.8–1.0 at 600 nm was reached. The cultures were cooled on ice to 20 °C and induced with 0.1 mM Isopropyl- $\beta$ -D-1-thiogalactopyranoside (IPTG), supplemented with 0.25 mM of CoCl<sub>2</sub>, and shaken for an additional 16 hours at 20 °C.

Cells were pelleted by centrifugation at  $6,370 \times g$  for 10 minutes at 4 °C in a Beckman Coulter Avanti JA-10 rotor and resuspended in buffer **A** (50 mM sodium phosphate buffer, pH 7.5, containing 300 mM NaCl, 5% glycerol, and 10 mM imidazole) at a ratio of 5 mL per gram of cells. Cells were lysed by ultrasonication (Misonix Sonicator 3000) for 4 min (alternating 30s on and 45s off) at 21 W. Cell lysate was separated from cell debris by centrifugation in a JA-20 rotor at  $31,000 \times g$  at 4 °C for 20 min. Cell lysate was purified using immobilized metal affinity chromatography (IMAC; 100 mg protein/5mL column) on a GE ÄKTA Fast Protein Liquid Chromatography (FPLC) system at 4 °C. The column was washed with 50 mL of buffer **A** followed by 50 mL of buffer **A** containing additional imidazole (35 mM). The protein was eluted using a linear gradient (0–100%) of buffer **B** (50 mM NaH<sub>2</sub>PO<sub>4</sub> pH 7.5, 300 mM NaCl, 10% glycerol, 525 mM imidazole) at a flow rate of 1 mL/min resulting in *MbNHase* being eluted between 150 to 240 mM imidazole.

Fractions containing WT *MbNHase* were pooled and concentrated to ~1 mL using an Amicon Ultra-15 (Millipore) and loaded onto a 16/60 Superdex 200 prep grade (GE Healthcare) polishing column using buffer **C** (50 mM HEPES and 300 mM NaCl at pH 8.0). Pure WT *MbNHase* was concentrated using an Amicon Ultra-15 (Millipore) and analyzed by SDS-PAGE with a 12.5% polyacrylamide SPRINT NEXT GEL™ (Amresco). Gels were stained with Gel Code Blue (Thermo-Fisher Scientific). The protein concentration of purified WT *MbNHase* was determined by measuring the absorbance at 280 nm on a Shimadzu UV-2450 spectrophotometer. The calculated molecular weight for the WT *MbNHase* homodimer is 111,207 g/mol with an extinction coefficient of  $143,700 \text{ cm}^{-1} \text{ M}^{-1}$ . The molecular weight is in good agreement with SDS-PAGE data [11].



Northampton, MA). Kinetic data for each *MbNHase* variant was determined more than three times for multiple purifications, all of which provided consistent results.

### Metal Analysis.

The metal content of WT *MbNHase* and each variant, expressed in the presence and absence of  $\text{CoCl}_2$ , was determined by inductively-coupled plasma mass spectrometry (ICP-MS). For comparison purposes, the Co-type NHase from *Pseudonocardia thermophila* JCM 3095 (*PtNHase*) was expressed and purified as previously described [20], and the metal content determined along with a buffer control that contained no protein. All protein samples were pretreated with 1 M urea and digested with concentrated nitric acid (0.863 mL) followed by heating at 70 °C for 1 h, allowed to cool to room temperature, and then diluted to a final concentration of 5% nitric acid. Samples were submitted for analysis at the Water Quality Center in the College of Engineering at Marquette University (Milwaukee, WI, USA).

### Electronic Absorption and Electron Paramagnetic Resonance Spectra.

Electronic absorption spectra were recorded on a Shimadzu UV-2450 spectrophotometer equipped with a TCC-240A temperature-controlled cell holder. Spectra for WT *MbNHase* and each variant as well as *PtNHase* were obtained at 25 °C in a 1 cm quartz cuvette in 50 mM HEPES buffer containing 300 mM NaCl, pH 8.0. X-band EPR spectra for WT *MbNHase* were recorded at 4 K, 0.1 mW in 50 mM HEPES buffer containing 300 mM NaCl, pH 8.0 on a Bruker EMXplus spectrometer equipped with an ER4116DM (~ 9.6 GHz) resonator, an Oxford Instruments ESR900 helium flow cryostat, and Oxford Instruments ITC503 temperature controller.

## Results and Discussion

### Proteolytic Cleavage of WT *MbNHase*.

Active, mature *MbNHase* was obtained when expressed in the absence of an ( $\epsilon$ ) protein or the *E. coli* GroES/EL molecular chaperones [11][13], whereas prokaryotic NHase activation appears to absolutely require an activator protein [14–16]. These findings beg the question: “how is *MbNHase* functionally expressed?” We hypothesized that the insert region, which contains a His<sub>17</sub> section, (Figure 1) plays a key role in metalcentre assembly and therefore, created three altered *MbNHase* enzymes targeting this insert region.

Purified WT *MbNHase* exhibits a single band at ~55 kDa on SDS-PAGE (Figure 2) and a  $k_{cat}$  value of  $131 \pm 3 \text{ s}^{-1}$  ( $K_m = 83 \pm 10 \text{ mM}$ ) in 50 mM Tris-HCl buffer pH 7.0 at 25 °C using acrylonitrile as the substrate, values that are indistinguishable from those reported previously (Table 1) [11]. Size-exclusion chromatography revealed that WT *MbNHase* exists primarily as an ( $\alpha\beta$ )<sub>2</sub> homodimer in solution, analogous to the  $\alpha_2\beta_2$  heterotetramer architecture observed for prokaryotic NHases. However, storage of WT *MbNHase* at 4 °C in 50 mM Tris-HCl buffer, pH 7.0 for approximately two weeks, provided an *MbNHase* enzyme with a modestly increased  $k_{cat}$  value of  $163 \pm 4 \text{ s}^{-1}$  but a similar  $K_m$  value of  $93 \pm 15 \text{ mM}$ , using acrylonitrile as the substrate (Table 1). SDS-PAGE analysis of aged *MbNHase* samples revealed two polypeptides of ~24 and ~26 kDa (Figure 2), while size exclusion chromatography suggested an  $\alpha_2\beta_2$  heterotetramer, identical to that observed for

prokaryotic NHases. These data suggested that WT *MbNHase* is cleaved, likely by trace amounts of proteases. The observed increase in  $k_{cat}$  for the proteolytically cleaved *MbNHase* enzyme, represents an ~20% increase in rate over WT *MbNHase*. The increased rate was very reproducible for batch-to-batch preparations, providing the calculated error of  $\pm 4 \text{ s}^{-1}$ . The observed increase in activity is perhaps due to an easing of conformational stress induced by the insert region in and around the active site, although structural characterization will be required to confirm this.

Confirmation of an  $\alpha_2\beta_2$  heterotetramer after proteolytic cleavage of WT *MbNHase* was obtained by MALDI-TOF mass spectroscopy (Figure 3). Two masses were clearly observed at 24,848 Da and 25,530 Da, values that are consistent with SDS-PAGE estimates (Figure 2) and correspond to the  $\alpha$ - and  $\beta$ -subunits of *MbNHase* based on sequence comparison with the prototypical Co-type *PbNHase* enzyme (Figure 4). The two MALDI-TOF MS peaks were of similar intensities, indicating a ~1:1  $\alpha$ : $\beta$  ratio. Interestingly, the observed molecular masses from MALDI-TOF MS suggests that a 5,226 Da peptide is lost after proteolytic cleavage, comparable to the size of the complete insert region of WT *MbNHase*. Attempts to isolate the cleaved fragment by gel-filtration were unsuccessful suggesting that the fragment is likely cleaved into small peptides by protease contaminants. Cleavage of *MbNHase* could be prevented by an additional gel-filtration purification step performed directly after IMAC; however, the addition of metal ion inhibitors such as EDTA or 1,10-phenanthroline had no effect on *MbNHase* cleavage. Addition of protease inhibitor cocktails, such as AEBSEF, resulted in precipitation of *MbNHase*. Taken together, these data indicate that the single polypeptide of freshly isolated WT *MbNHase*, which contains fused  $\alpha$ - and  $\beta$ -subunits linked by an insert region, is cleaved into separate  $\alpha$ - and  $\beta$ -subunits upon ageing, likely by trace amounts of proteases, resulting in a modestly more active  $\alpha_2\beta_2$  heterotetrameric form of *MbNHase*.

A combination of UV-Vis and EPR spectroscopy coupled with metal analyses was used to determine that the proteolytically cleaved *MbNHase* enzyme contained its full complement of Co(III). ICP-MS data indicated that the proteolytically cleaved *MbNHase* enzyme contained  $1.9 \pm 0.1$  equivalents of cobalt per  $\alpha_2\beta_2$  heterotetramer, indistinguishable from WT *MbNHase* (Table 1) with no other metal ions detected above the background level of <10 ppb [11]. Proteolytically cleaved *MbNHase* exhibited the typical amber color of Co-type NHase enzymes in 50 mM HEPES buffer containing 300 mM NaCl, pH 8.0 (Figure 5) [1], and the UV-Vis spectrum reveals the characteristic  $S \rightarrow \text{Co(III)}$  ligand-to-metal-charge-transfer (LMCT) band at 315 nm ( $\epsilon = 2,500 \text{ M}^{-1} \text{ cm}^{-1}$ ) (Figure 5), which is blue-shifted by ~10 nm compared to WT *MbNHase* [11]. EPR spectra show no detectable Co(II) signals consistent with the presence of low-spin Co(III), which is diamagnetic (Figure SI-2). These data indicate that proteolytically cleaved *MbNHase*, retains its full complement of Co(III) and that neither the insert region nor the (His)<sub>17</sub> motif is required for catalysis in the proteolytically cleaved *MbNHase* enzyme.

### Examination of the functional role of the (His)<sub>17</sub> insert.

To investigate whether the (His)<sub>17</sub> region plays a role in metal ion insertion and/or the posttranslational modification of the active site, the *MbNHase*<sup>238–257</sup> (His)<sub>17</sub> deletion



mutant, was prepared. SDS-PAGE analysis revealed two bands at ~25.5 and ~28.5 kDa for *MbNHase*<sup>238–257</sup> while size-exclusion chromatography indicated that *MbNHase*<sup>238–257</sup> exists primarily as an  $\alpha_2\beta_2$  heterotetramer with a molecular weight of ~108 kDa, much like prokaryotic Co-type NHases (Figure 6). Kinetic analyses of the *MbNHase*<sup>238–257</sup> (His)<sub>17</sub> deletion mutant, expressed in the absence or presence of the prototypical Co-type activator ( $\epsilon$ ) protein, *PtNHase*<sup>act</sup>, using acrylonitrile as the substrate, were performed in triplicate for multiple purifications in 50 mM Tris-HCl buffer, pH 7.0 at 25 °C providing  $k$  values of  $71 \pm 4 \text{ s}^{-1}$  and  $166 \pm 5 \text{ s}^{-1} \text{ cat}$  respectively.  $K_m$  values for the *MbNHase*<sup>238–257</sup> (His)<sub>17</sub> deletion mutant expressed in the absence or presence of the *PtNHase*<sup>act</sup> were  $104 \pm 17 \text{ mM}$  and  $125 \pm 17 \text{ mM}$ , respectively (Table 1). The *MbNHase*<sup>238–257</sup> (His)<sub>17</sub> deletion mutant expressed in the absence or presence of *PtNHase*<sup>act</sup> contained  $1.8 \pm 0.1$  and  $2.3 \pm 0.2$  equivalents of cobalt per  $\alpha_2\beta_2$  heterotetramer, respectively, with no other metal ions detected above the background level of <10 ppb. The *MbNHase*<sup>238–257</sup> (His)<sub>17</sub> deletion mutant expressed in either the absence or presence of *PtNHase*<sup>act</sup> in 50 mM HEPES buffer containing 300 mM NaCl, pH 8.0 exhibited the characteristic S  $\rightarrow$  Co(III) LMCT band at ~320 nm ( $\epsilon = 2,200 \text{ M}^{-1} \text{ cm}^{-1}$ ) (Figure 5), nearly identical to WT *MbNHase* [11]. While the (His)<sub>17</sub> region is not required for metal uptake or active site maturation, expression in the presence of the prototypical prokaryotic activator protein, *PtNHase*<sup>act</sup>, does enhance the observed  $k_{\text{cat}}$  value by ~60%, which is greater than would be expected from the slight increase (~20%) in metal content. Therefore, *PtNHase*<sup>act</sup> does assist in the activation of the *MbNHase*<sup>238–257</sup> (His)<sub>17</sub> deletion mutant but is not required for post-translational modification of the active enzyme.

#### Investigation of the Insert region of MbNHase.

The *MbNHase*<sup>219–272</sup> insert region deletion mutation provides an enzyme with the entire insert region between the  $\alpha$  and  $\beta$  regions of WT *MbNHase* removed (Figure 1). Removal of this insert region essentially converts the eukaryotic *MbNHase* into a prokaryotic NHase analog, allowing the direct comparison of *MbNHase*<sup>219–272</sup> and *PtNHase*. The *MbNHase*<sup>219–272</sup> insert region deletion mutant expressed in the absence of *PtNHase*<sup>act</sup> exhibited two bands on SDS-PAGE at ~25.5 and ~26.5 kDa. Size-exclusion chromatography indicated that *MbNHase*<sup>219–272</sup> exists primarily as an  $\alpha_2\beta_2$  heterotetramer with a molecular weight of ~104 kDa, indistinguishable from proteolytically cleaved WT *MbNHase* and prokaryotic Co-type NHases such as *PtNHase*. Surprisingly, co-expression of *MbNHase*<sup>219–272</sup> in the presence of *PtNHase*<sup>act</sup> yielded a single band at ~52 kDa on SDS-PAGE which is consistent with an  $\alpha\beta$  complex. However, it could also be due to the formation of an  $\alpha(\epsilon)_2$  complex as *PtNHase*<sup>act</sup> is ~14 kDa so an  $\alpha(\epsilon)_2$  complex would have a mass of ~53.5 kDa. Interestingly, the Co-type ( $\epsilon$ ) protein from *Rhodococcus rhodochrous* J1 was shown to form an  $\alpha(\epsilon)_2$  complex, which was proposed to bind Co(II) and insert it into apo- $\alpha_2\beta_2$  NHase *via* a “self-subunit swapping” mechanism [21]. The Co-type ( $\epsilon$ ) protein was also proposed to facilitate oxidation of two active site Cys-residues. Attempts to separate the ~52 kDa proteins into their individual components were unsuccessful even in the presence of 8 M urea, 1 M dichlorodiphenyltrichloroethane (DDT) or SDS at 95 °C for 10 min (Figure 7).

Kinetic analysis of the *MbNHase*<sup>219–272</sup> insert region deletion mutant expressed in the absence or presence of *PtNHase*<sup>act</sup> in 50 mM Tris-HCl buffer, pH 7.0 at 25 °C provided  $k_{cat}$  values of  $75 \pm 8 \text{ s}^{-1}$  and  $117 \pm 10 \text{ s}^{-1}$ , respectively, using acrylonitrile as the substrate (Table 1). These kinetic data suggest that the *MbNHase*<sup>219–272</sup> insert region deletion mutant expressed in the presence of *PtNHase*<sup>act</sup>, is likely an  $\alpha\beta$  complex, even so, the Co-type NHase ( $\epsilon$ ) proteins are known to have significant sequence identity with the NHase  $\beta$ -subunit [22, 23], so  $\alpha(\epsilon)_2$  complex might be expected to be catalytically competent, but not likely more active than an  $\alpha_2\beta_2$  heterotetramer such as was observed for the *MbNHase*<sup>D</sup> insert region deletion mutant expressed in the absence of *PtNHase*<sup>act</sup>. The *MbNHase*<sup>219–272</sup> insert region deletion mutant expressed in the absence or presence of *PtNHase*<sup>act</sup> is not particularly stable in 50 mM Tris-HCl buffer, pH 7.0 at 25 °C and loses > 95% of its activity over the course of a few hours, indicating that the insert region plays a role in stabilizing the WT *MbNHase* enzyme. The *MbNHase*<sup>219–272</sup> insert region deletion mutant contained  $1.7 \pm 0.1$  equivalents of cobalt per  $\alpha_2\beta_2$  heterotetramer, irrespective of the co-expression of *PtNHase*<sup>act</sup>, a value nearly identical to that observed for WT *MbNHase* (Table 1). UV-Vis spectra of the *MbNHase*<sup>219–272</sup> insert region deletion mutant expressed in the absence or presence of *PtNHase*<sup>act</sup> in 50 mM HEPES buffer containing 300 mM NaCl, pH 8.0 were indistinguishable from each other and WT *MbNHase* (Figure 5). Therefore, *MbNHase*<sup>238–257</sup> binds its full complement of Co(III) ions without the assistance of an ( $\epsilon$ ) protein, indicating that the insert region is also not required for metal ion binding or active site maturation.

## Conclusion

Characterization of the eukaryotic NHase from *Monosiga brevicollis* constructs described herein, confirm that *MbNHase* does not require an NHase activator protein or the *E. coli* chaperone proteins GroEL/ES for metalcentre assembly, including metal ion insertion and active site post-translational maturation. In addition, these data indicate that the (His)<sub>17</sub> region found within the insert that links the  $\alpha$ - and  $\beta$ -subunits is not required for metal ion incorporation or active site maturation. The fact that the proteolytically cleaved WT *MbNHase* enzyme and the *MbNHase*<sup>238–257</sup> (His)<sub>17</sub> deletion mutant each exhibit a modest increase in activity compared to WT *MbNHase*, suggests that the insert region likely induces a structural strain on the active site that has a limiting effect on the catalytic rate of hydration. The lack of the need for either an intrinsic or an extrinsic activator polypeptide for *MbNHase* is in stark contrast to the absolute requirement for an activator for assembly and activation of the otherwise similar prokaryotic NHases. The pertinent and related outstanding questions are, “How can the *MbNHase* metalcentre self-assemble and self-activate?” and, “Why do the prokaryotic NHase metallocenters require activators for assembly and activation?” The genetically engineered functional constructs of *MbNHase* described herein represent an important new tool with which to further address these important questions using structural and spectroscopic methods.

## Supplementary Material

Refer to Web version on PubMed Central for supplementary material.



## Acknowledgments

This work was supported by National Science Foundation (CHE-1808711, RCH and BB; CHE-1532168 BB & RCH), the Todd Wehr Foundation, Bruker Biospin, and the National Institutes of Health/NIBIB National Biomedical EPR Center (P41-EB001980).

## Abbreviations.

<b>NHase</b>	nitrile hydratase
<b>ORF</b>	open reading frame
<b>ICP-MS</b>	inductively-coupled plasma mass spectrometry
<b>IMAC</b>	immobilized metal affinity chromatography

## References

1. Kovacs JA (2004) *Chem Rev* 104:825–848 [PubMed: 14871143]
2. Harrop TC and Mascharak PK (2004) *Acc Chem Res* 37:253–260 [PubMed: 15096062]
3. Kobayashi M, Nagasawa T and Yamada H (1992) *Trends Biotechnol* 10:402–408 [PubMed: 1368882]
4. Nagasawa T, Shimizu H and Yamada H (1993) *Appl Microbiol Biotechnol* 40
5. Nagasawa T and Yamada H (1995) *Pure Appl Chem* 67:1241–1256
6. Yamada H and Kobayashi M (1996) *Biosci Biotech Biochem* 60:1391–1400
7. Prasad S and Bhalla TC (2010) *Biotechnology Advances* 28:725–741 [PubMed: 20685247]
8. Nagasawa T, Mathew CD, Mauger J and Yamada H (1988) *Appl Environ Microbiol* 54:1766–1760 [PubMed: 16347686]
9. Marron AO, Akam M and Walker G (2012) *PLoS ONE* 7:e32867 [PubMed: 22505998]
10. Foerster KU, Doerks T, Muller J, Raes J and Bork P (2008) *PLoS ONE* 3:e3976 [PubMed: 19096720]
11. Martinez S, Yang X, Bennett B and Holz RC (2017) *Biochimica et Biophysica Acta (BBA) - Proteins and Proteomics* 1865:107–112 [PubMed: 27693250]
12. Tsujimura M, Odaka M, Nakayama H, Dohmae N, Koshino H, Asami T, Hoshino M, Takio K, Yoshida S, Maeda M and Endo I (2003) *J Am Chem Soc* 125:11532–11538 [PubMed: 13129355]
13. Dey A, Chow M, Taniguchi K, Lugo-Mas P, Davin S, Maeda M, Kovacs JA, Odaka M, Hodgson KO, Hedman B and Solomon EI (2006) *J Am Chem Soc* 128:533 – 541 [PubMed: 16402841]
14. Nishiyama M, Horinouchi S, Kobayashi M, Nagasawa T, Yamada H and Beppu T (1991) *J Bacteriol* 173:2465–2472 [PubMed: 2013568]
15. N. Hashimoto Y, M., Horinouchi S, Beppu T (1994) *Bioscience, biotechnology, and biochemistry* 58:1859–1869
16. Nojiri M, Yohda M, Odaka M, Matsushita Y, Tsujimura M, Yoshida T, Dohmae N, Takio K and Endo I (1999) *Journal of Biochemistry* 125:696–704 [PubMed: 10101282]
17. Mendel RR, Smith AG, Marquet A and Warren MJ (2007) *Natural Product Reports* 24:963–971 [PubMed: 17898892]
18. Higgins KA, Carr CE and Maroney MJ (2012) *Biochemistry* 51:7816–7832 [PubMed: 22970729]
19. Stevens JM, Rao Saroja N, Jaouen M, Belghazi M, Schmitter J-M, Mansuy D, Artaud I and Sari M-A (2003) *Protein Expression and Purification* 29:70–76 [PubMed: 12729727]
20. Martinez S, Wu R, Sanishvili R, Liu D and Holz R (2014) *Journal of the American Chemical Society* 136:1186–1189 [PubMed: 24383915]
21. Zhou Z, Hashimoto Y, Cui T, Washizawa Y, Mino H and Kobayashi M (2010) *Biochemistry* 49:9638–9648 [PubMed: 20886813]

22. Zhou Z, Hashimoto Y and Kobayashi M (2009) *The Journal of Biological Chemistry* 284:14930–14938 [PubMed: 19346246]
23. Zhou Z, Hashimoto Y, Shiraki K and Kobayashi M (2008) *Proceedings of the National Academy of Sciences* 105:14849–14854

Author Manuscript

Author Manuscript

Author Manuscript

Author Manuscript

### Highlights

- Metallocentre assembly in the eukaryotic nitrile hydratase from *Monosiga brevicollis* (*MbNHase*).
- WT *MbNHase* expresses as a single polypeptide with fused  $\alpha$ - and  $\beta$ -subunits linked by a (His)<sub>17</sub> and an insert region.
- Two insert region mutant *MbNHase* enzymes were examined, *MbNHase*<sup>238–257</sup> and *MbNHase*<sup>219–272</sup>.
- Neither the (His)<sub>17</sub> nor the entire insert region are required for metallocentre assembly and maturation.

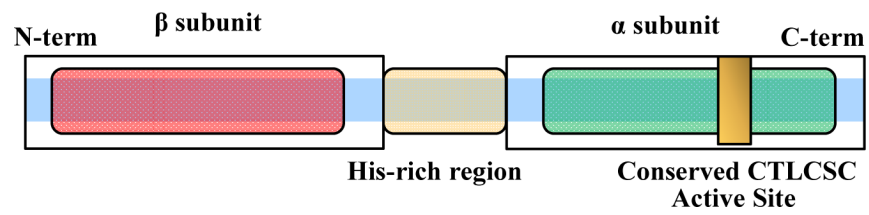


**Figure 1.**  
Scheme showing the arrangement of the NHase  $\beta$ - and  $\alpha$ -subunits in eukaryotes.

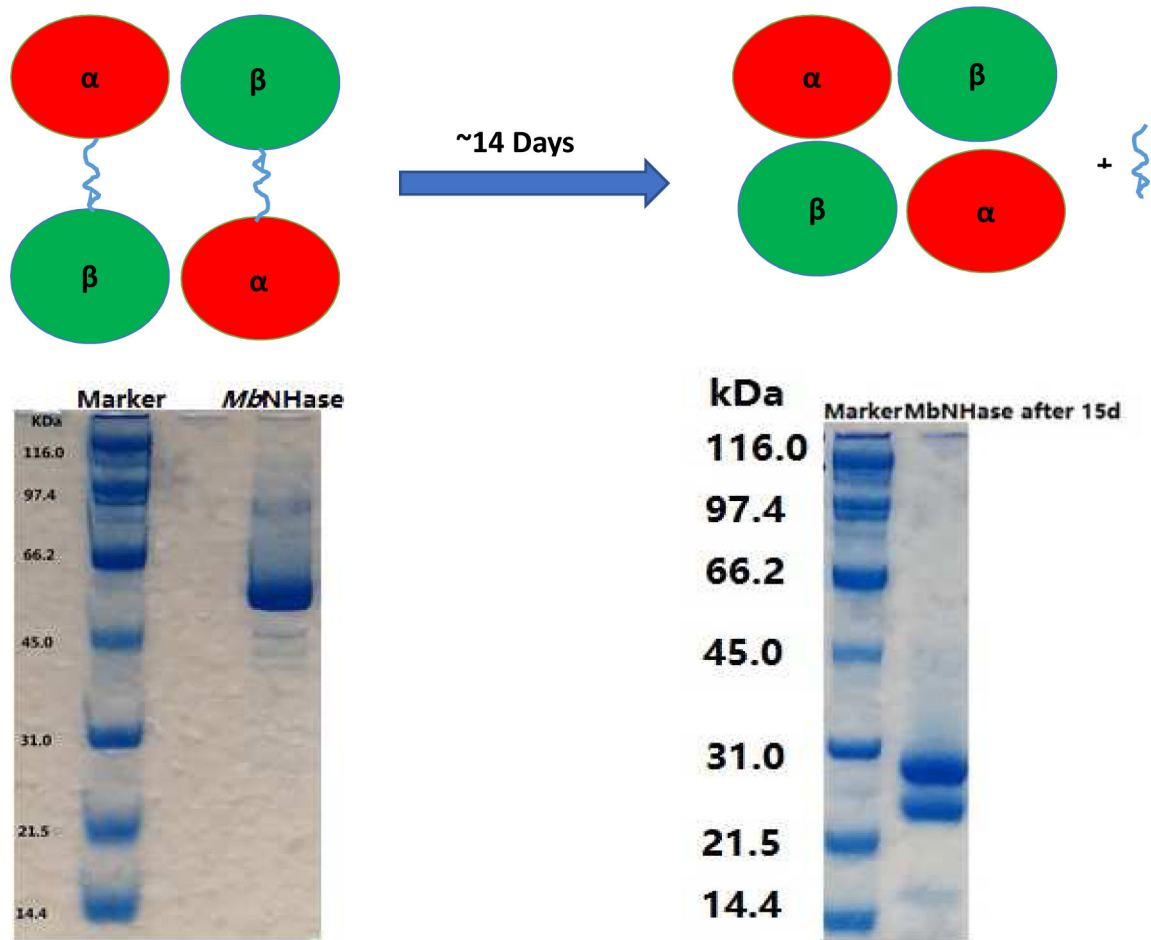


**Figure 2.** The SDS-PAGE of (a) WT *MbNHase* and (b) the proteolytically cleaved *MbNHase* enzyme.

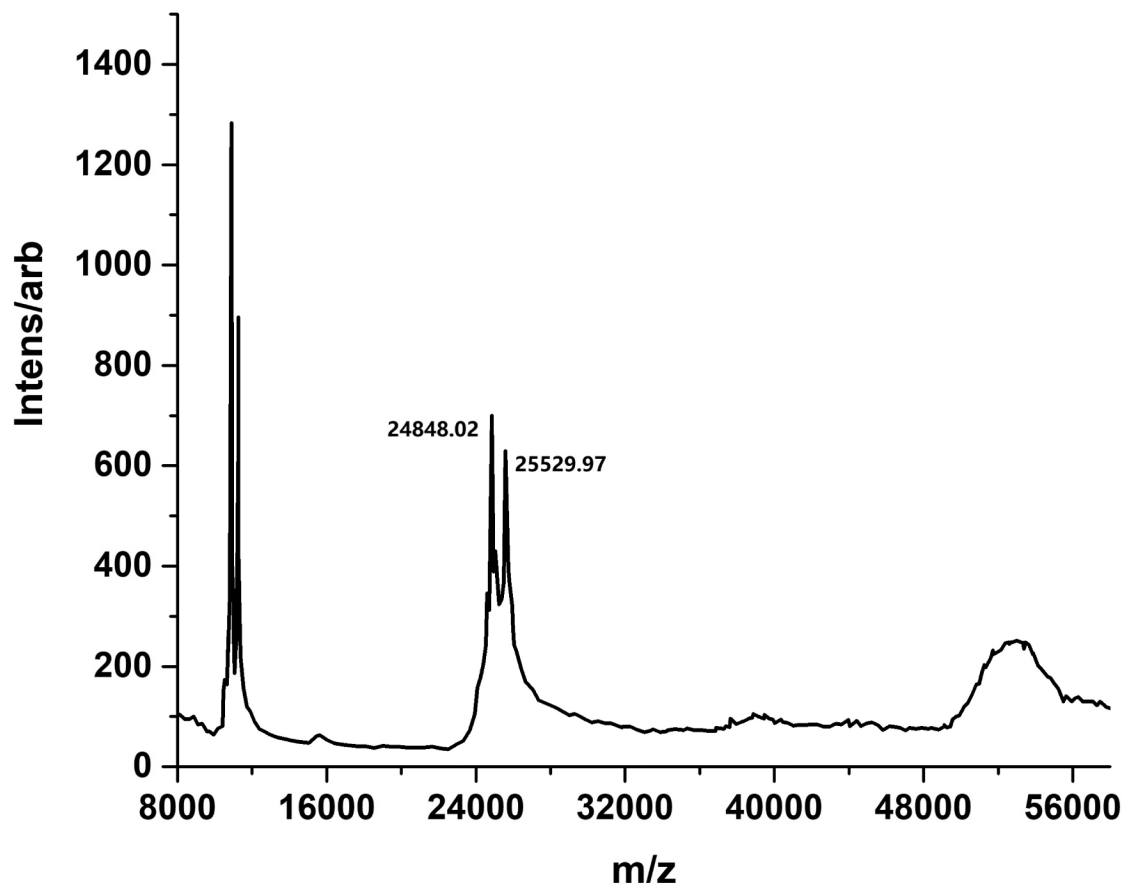


**Figure 3.** MALDI-TOF Mass Spectra of proteolytically cleaved *Mb*NHase revealing two peaks at 24.8 and 25.5 kDa corresponding to independent  $\alpha$ - and  $\beta$ -subunits.



A9V2C1	MbNHase	1	MHLFTYDLHHDVGGAEENMLRPLDRHE-RDYLPWERHIIHALVLLVKQGRMSVDELRRGV	59
Q7SID3	PtNHase β	1	-----MNGVYDVGGTDGLGPIINRPADEPVFRAEWKVAFAFMPATFRAGFMGLDEFRRFGI	55
Q7SID2	PtNHase α	1	-----	0
A9V2C1	MbNHase	60	EGLPSSLAEQASYEKWGLSVSRILTEKGTVSGHELEQG-----	98
Q7SID3	PtNHase β	56	EQMNPAAEYLESPYYWHWIRTYIHGGVVRGKIDLEELERRTQYYRENPDAPLPEHEQKPEL	115
Q7SID2	PtNHase α	1	-----	0
A9V2C1	MbNHase	99	-----FLGVPT-TDLQVPRFQVQQRVMVRFPGTTFAYRQPHLRVPGYVHGAVGTIV	149
Q7SID3	PtNHase β	116	IEFVNQAVYGGPLASREVDKPKFKEGDVVRF-----STASPKGHARRARYVRGKTGTVV	170
Q7SID2	PtNHase α	1	-----	0
A9V2C1	MbNHase	150	ELPGLFQDPMTGAYGERGTAQPLRYVAFSHRALWPEGAAHAEPGELEDGVVVDVSQPWLE	209
Q7SID3	PtNHase β	171	KHHGAYIYPTAGNGLGCEPEHLYTVRFQAQELWGPEG-----DPNSSVYYDCWEPYIE	224
Q7SID2	PtNHase α	1	-----	0
A9V2C1	MbNHase	210	ALSEADYQRLATLHRVAFTPDSNPPQA <span style="background-color: yellow;">KHHHHHHHHHDDHHHHHHHHH</span> <span style="background-color: green;">AMHAEHEAHTHD.</span>	269
Q7SID3	PtNHase β	225	LVDTKAAAA-	233
Q7SID2	PtNHase α	1	-----	0
A9V2C1	MbNHase	270	<span style="background-color: green;">TRY</span> GTEQAAVAKEAALDFPYQPWCEALVQTLTRRGVVRSDDELHATLASLDALQNSGAGPQ	329
Q7SID3	PtNHase β	234	---	233
Q7SID2	PtNHase α	1	---MTENILRKSDEEIQKEITARVKALESMLIEQGILTTSMIDRMAEYENEVGPHLGAK	57
A9V2C1	MbNHase	330	LVARAWSDAAFAEWLLTDAAAAASLAIRTTNYDADPASAERVGGHRLFSHNHTELRVVA	389
Q7SID3	PtNHase β	234	-----	233
Q7SID2	PtNHase α	58	VVKAWTDPEFKRLLADGTEACKELGIGL-----QGEDMMWVE	97
A9V2C1	MbNHase	390	NTDVTNHLVGV <span style="background-color: orange;">TTLCSYPT</span> TAILGLSPWYKSKVFRARAVREPRRLREEFGLVLPARGI	449
Q7SID3	PtNHase β	234	-----	233
Q7SID2	PtNHase α	98	NTDEVHVVV <span style="background-color: orange;">TTLCSYPT</span> WVVLGLPPNWFKEPQYRSRVVREPRQLLKEEFGEVPPSKEI	157
A9V2C1	MbNHase	450	RVHDSTADLRYMVLQRPQGTGEGWSEEHLRTIVTRDSSLGTAVPRVD	496
Q7SID3	PtNHase β	234	-----	233
Q7SID2	PtNHase α	158	KVWDSSSEMRFVVLQRPAGTDGWSEEELATLVTRRESMIGVEPAKAV	204

**Figure 4.** Sequence alignment of *Mb*NHase and *Pt*NHase shows that the α-subunits share 23% identity while the β-subunits exhibit 32% identity (Orange: active site; green: insert region; yellow: histidine rich region).

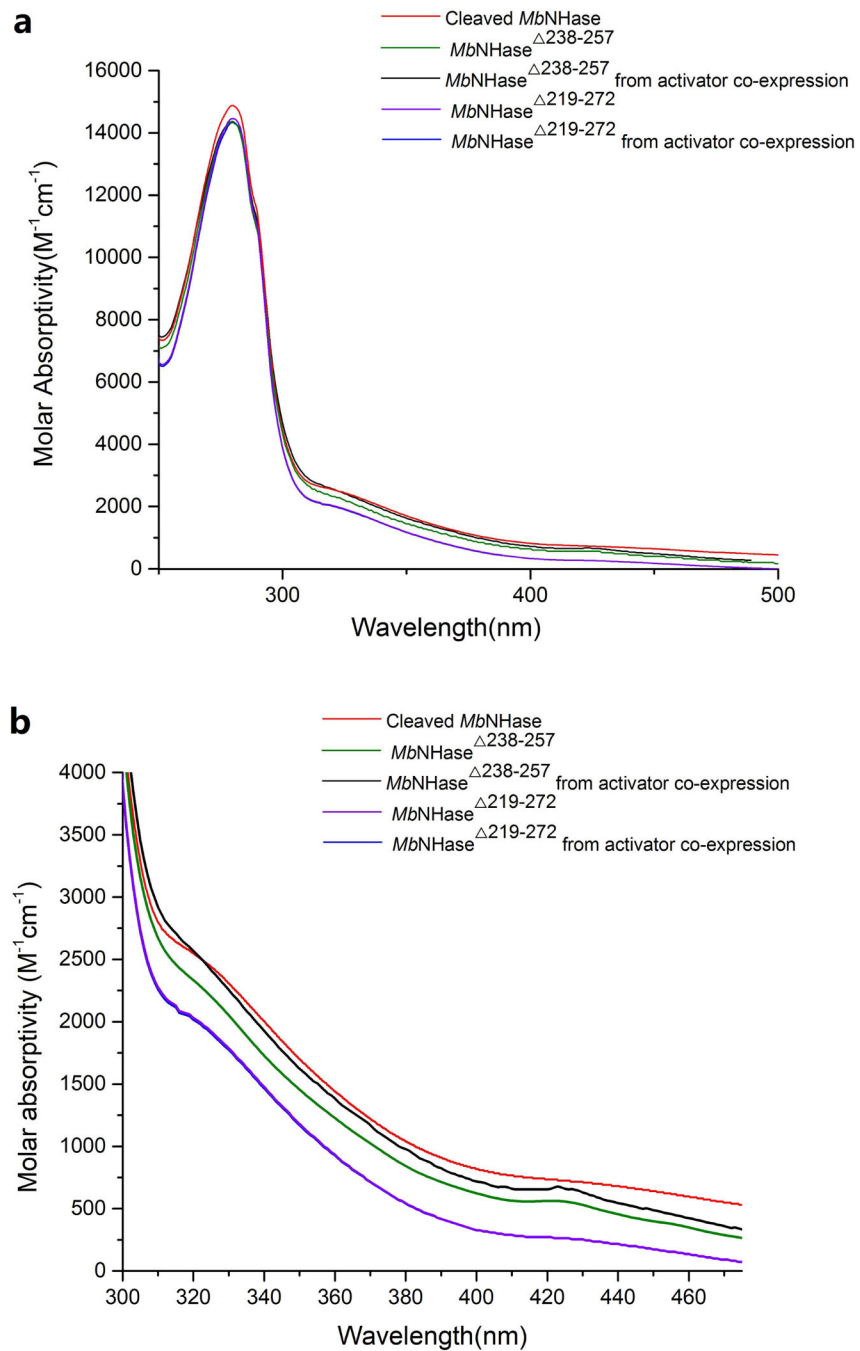


**Figure 5.** UV-Vis spectra of various *MbNHase* constructs between (a) 280 and 500 nm; (b) 300 and 480 nm in 50 mM HEPES buffer containing 300 mM NaCl at pH 8.0. (b)

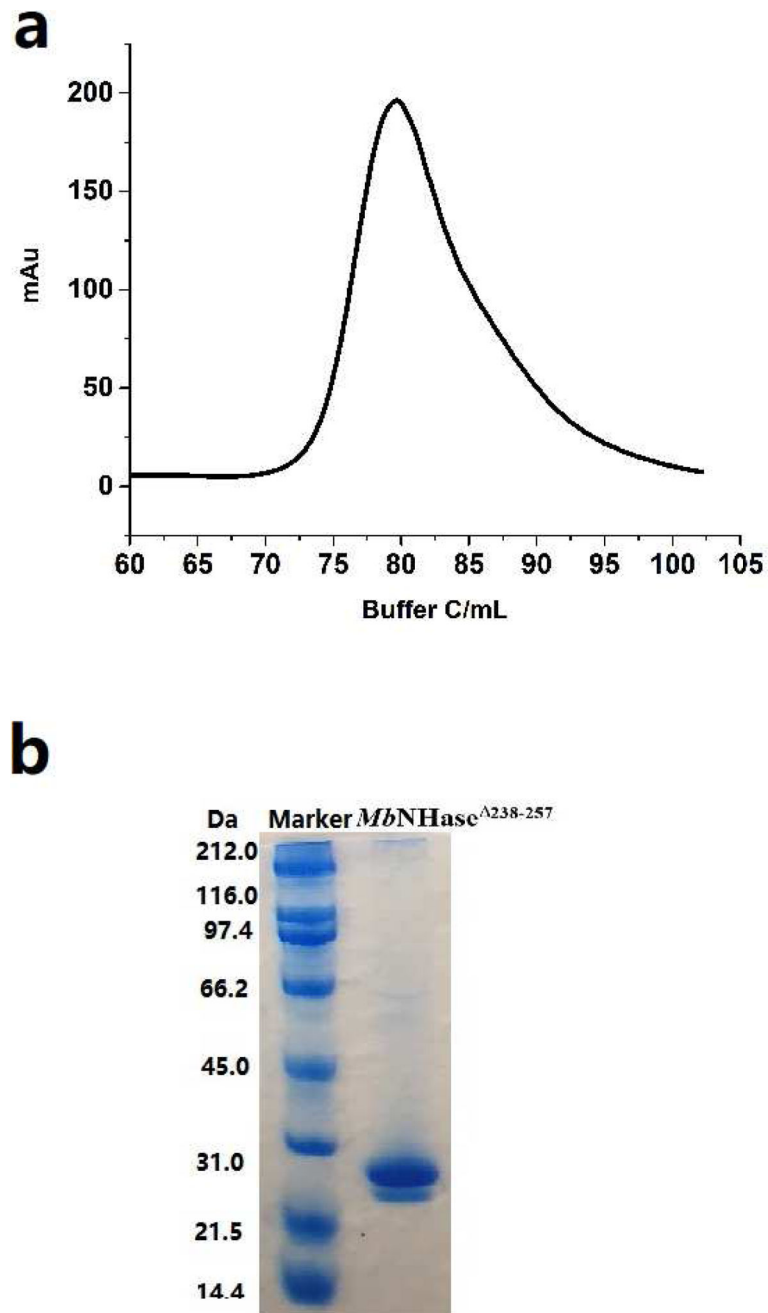


**Figure 6.** Purification of the *MbNHase*<sup>238–268</sup> mutant. a) size-exclusion column indicating a single peak corresponding to an  $\alpha_2\beta_2$  heterotetramer; b) SDS-PAGE gel page showing that the purified  $\alpha$  and  $\beta$ -subunits are two independent proteins.

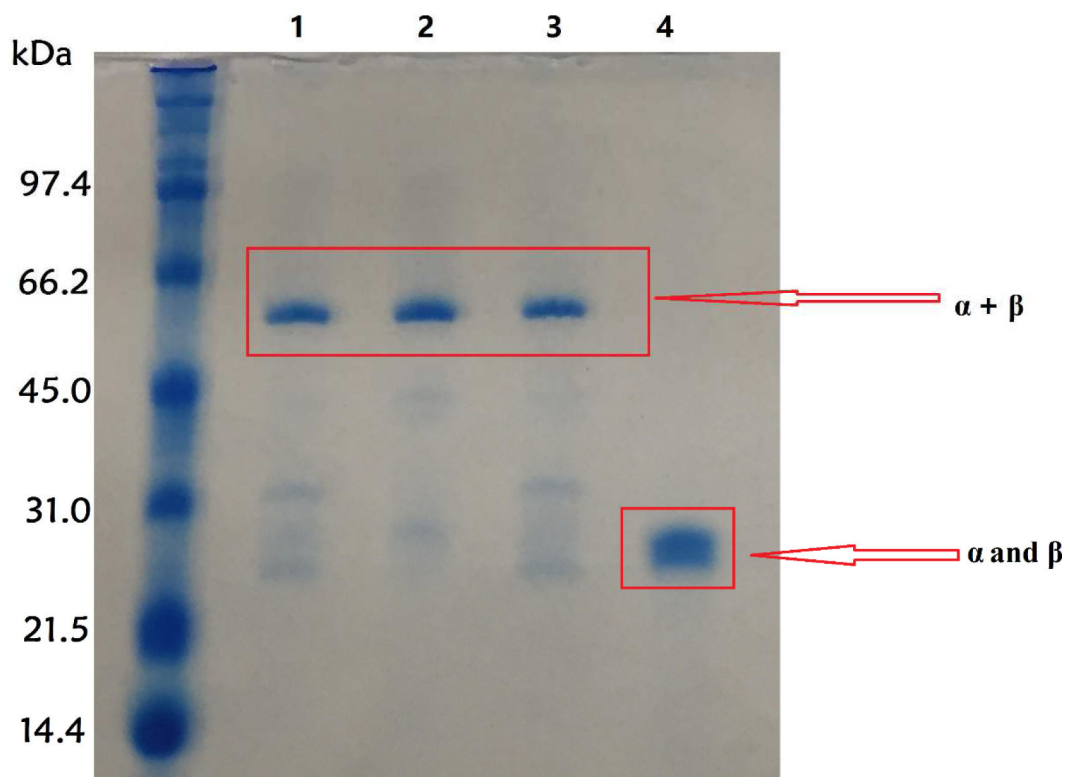


**Figure 7.** SDS-PAGE gel of *MbNHase*<sup>219-272</sup>. Column 1: *MbNHase*<sup>219-272</sup> from activator co-expression; Column 2: *MbNHase*<sup>219-272</sup> from *PtNHase* activator co-expression treated by 8mM Urea; Column 3: *MbNHase*<sup>219-272</sup> from activator co-expression treated by 8M urea and 1M DDT; Column 4: *MbNHase*<sup>D219-272</sup> without activator.

**Table 1.**Kinetic constants for the wild-type and mutant *MbNHases*<sup>a</sup>

	$k_{cat}$ (s <sup>-1</sup> )	$K_m$ (mM)	$k_{cat}/K_m$ (s <sup>-1</sup> mM <sup>-1</sup> )	Metal Content
Wild-type <sup>b</sup>	131 ± 3	83 ± 10	1.6	1.8 ± 0.1
Cleaved	163 ± 4	93 ± 15	1.8	1.9 ± 0.1
238–257	71 ± 4	104 ± 17	0.7	1.8 ± 0.1
238–257 + <i>PtNHase</i> <sup>act</sup>	166 ± 5	125 ± 17	1.3	2.3 ± 0.2
219–272	75 ± 8	73 ± 14	1.0	1.7 ± 0.1
219–272 + <i>PtNHase</i> <sup>act</sup>	117 ± 10	149 ± 23	0.8	1.7 ± 0.1

<sup>a</sup>Acrylonitrile was used as the substrate.<sup>b</sup>Reference [11].